

## Supporting Information

### A Simple Approach to Prepare Chlorinated Polymer Donors with Low-lying HOMO Level for High Performance Polymer Solar Cells

Beibei Qiu,<sup>a,b</sup> Shanshan Chen,<sup>c</sup> Hongneng Li,<sup>a</sup> Zhenghui Luo,<sup>a</sup> Jia Yao,<sup>a</sup> Chenkai Sun,<sup>a,b</sup>  
Xiaojun Li,<sup>a,b</sup> Lingwei Xue,<sup>a</sup> Zhi-Guo Zhang,<sup>a</sup> Changduk Yang,<sup>c</sup> Yongfang Li<sup>a,b,d,\*</sup>

<sup>a</sup> Beijing National Laboratory for Molecular Sciences, CAS Key Laboratory of Organic Solids, Institute of Chemistry, Chinese Academy of Sciences, Beijing 100190, China

<sup>b</sup> School of Chemical Science, University of Chinese Academy of Sciences, Beijing 100049, China

<sup>c</sup> Department of Energy Engineering, School of Energy and Chemical Engineering, Low Dimensional Carbon Materials Center, Ulsan National Institute of Science and Technology (UNIST), Ulsan 689-798, South Korea

<sup>d</sup> Laboratory of Advanced Optoelectronic Materials, College of Chemistry, Chemical Engineering and Materials Science, Soochow University, Suzhou, Jiangsu 215123, China

\* Corresponding authors: [liyf@iccas.ac.cn](mailto:liyf@iccas.ac.cn) (Y. Li)

### Experimental Section

#### Materials

Compound 4,8-Dihydrobenzo[1,2-b:4,5-b']dithiophen-4,8-dione (BDT) was bought from Derthon Optoelectronic Materials Science Technology Co LTD. Pd(PPh<sub>3</sub>)<sub>4</sub> was obtained from J&K chemical Co. Compounds 1a, 1b, 2a and 2b (see Scheme 1) were synthesized according to the previous literatures. Toluene was dried over Na/benzophenone and freshly distilled prior to use. The other chemicals, solvents and materials used in this work were all commercially available and used without further purification.

Scheme 1 shows the synthetic routes of **J11** and **J12**. The detailed synthesis processes are described in the following:

#### Synthesis of **3a**

Under protection of argon, to a solution of Compound **2a** (2.3 g, 10 mmol) in 50 mL of THF, LDA (2 M, 5.0 mL) was added dropwise at -78 °C. The mixture was stirred for 1 hour and subsequently warmed to room temperature. Then benzo[1,2-b:4,5-

b0]dithiophene-4,8-dione (0.88 g, 4 mmol) was added. The reaction was then stirred at 50 °C for 2 h. After that, a mixture of SnCl<sub>2</sub>·2H<sub>2</sub>O (6.3 g, 28 mmol) in 10% HCl (14 mL) was added into the mixture at room temperature and stirred over night at ambient temperature. The mixture was then poured slowly into ice water and extracted with CH<sub>2</sub>Cl<sub>2</sub>, and the combined organic phases were concentrated to obtain the crude product. Solvent was removed under reduced pressure and the residue was purified by silica gel column chromatography using petroleum ether as eluent to afford compound **3a** as a pale yellow solid (1.56 g, 60%).

<sup>1</sup>H NMR (300 MHz, CDCl<sub>3</sub>): δ 7.61 (d, *J* = 5.7 Hz, 2H), 7.48 (d, *J* = 5.7 Hz, 2H), 7.17 (s, 2H), 2.68 (t, *J* = 7.5 Hz, 4H), 1.75-1.60 (m, 4H), 1.49-1.19 (m, 20H), 0.89 (t, *J* = 6.2 Hz, 6H).

<sup>13</sup>C NMR (75 MHz, CDCl<sub>3</sub>): δ 139.79, 139.13, 136.56, 135.83, 128.87, 128.03, 125.49, 123.38, 123.07, 31.89, 29.63, 29.41, 29.29, 29.28, 28.13, 22.70, 14.14.

#### *Synthesis of 3b*

Compound **3b** was synthesized with similar method as that described above for the synthesis of **3a**, and a pale yellow solid was obtained (1.50 g, 55%).

<sup>1</sup>H NMR (300 MHz, CDCl<sub>3</sub>): δ 7.61 (d, *J* = 5.7 Hz, 2H), 7.50 (d, *J* = 5.7 Hz, 2H), 7.15 (s, 2H), 4.13 (t, *J* = 6.5 Hz, 4H), 1.90-1.75 (m, 4H), 1.60-1.21 (m, 21H), 0.88 (d, *J* = 6.7 Hz, 6H).

<sup>13</sup>C NMR (75 MHz, CDCl<sub>3</sub>): δ 152.21, 139.15, 136.53, 134.04, 128.29, 123.49, 122.94, 118.44, 109.44, 72.52, 31.82, 29.55, 29.34, 29.24, 25.85, 22.68, 14.12.

#### *Synthesis of M1*

Under protection of argon, to a solution of Compound **3a** (1.3 g, 2 mmol) in 50 mL of THF, LDA (2 M, 3 mL) was added dropwise at -78 °C. After the addition, the mixture was stirred for 2 hour. Then trimethyltin chloride (1 M in THF, 7 ml) was added in one portion and stirred over night at ambient temperature. Then, it was poured into water and extracted with CH<sub>2</sub>Cl<sub>2</sub>, washed by water and brine and after drying over MgSO<sub>4</sub>, the solvent was removed and the residue was recrystallized with methanol to afford a yellow solid (1.56 g, 80%).

<sup>1</sup>H NMR (300 MHz, CDCl<sub>3</sub>): δ 7.62-7.49 (m, 2H), 7.09 (s, 2H), 2.62 (t, *J* = 7.5 Hz, 4H), 1.69-1.53 (m, 4H), 1.46-1.09 (m, 20H), 0.81 (t, *J* = 6.6 Hz, 6H), 0.51-0.17 (m, 18H).

<sup>13</sup>C NMR (75 MHz, CDCl<sub>3</sub>): δ 143.38, 143.24, 139.67, 137.35, 136.56, 130.69, 128.79, 125.12, 121.66, 31.95, 29.64, 29.49, 29.31, 29.29, 28.15, 22.70, 14.16, -8.27.

#### *Synthesis of M2*

**M2** was synthesized with similar method as that described above for the synthesis of **M1**, and a yellow solid was obtained (1.51 g, 75%).

$^1\text{H}$  NMR (300 MHz,  $\text{CDCl}_3$ ):  $\delta$  7.70-7.57 (m, 2H), 7.15 (s, 2H), 4.15 (t,  $J = 6.6$  Hz, 4H), 1.90-1.77 (m, 4H), 1.56-1.24 (m, 20H), 0.88 (d,  $J = 6.8$  Hz, 6H), 0.56-0.29 (m, 18H).

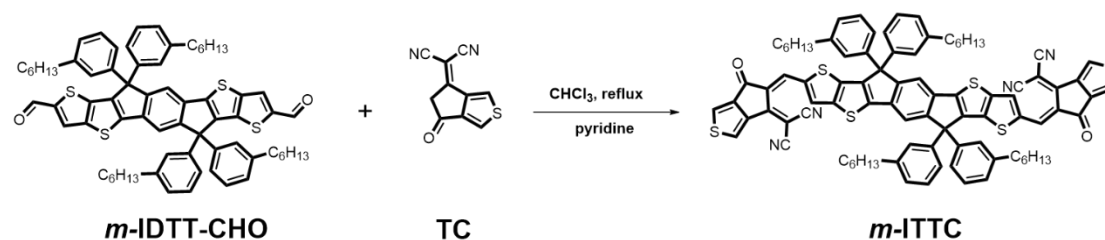
$^{13}\text{C}$  NMR (75 MHz,  $\text{CDCl}_3$ ):  $\delta$  152.11, 143.67, 143.41, 137.35, 134.83, 130.49, 121.75, 118.32, 109.04, 72.46, 31.83, 29.56, 29.37, 29.25, 25.87, 22.67, 14.12, -8.25.

### Synthesis of **J11**

A solution of **M1** (146 mg, 0.15 mmol), **M3** (105 mg, 0.15 mmol) in dry toluene (10 mL) was put into a two-necked flask. The solution was flushed with Ar for 20 min and  $\text{Pd}(\text{PPh}_3)_4$  (8 mg) was added into the flask. The solution was flushed with Ar again for 20 min. The oil bath was carefully heated to 110 °C and the reactant was stirred for 24 h at this temperature. After the reaction mixture was cooled to room temperature, the mixture was poured into methanol (150 mL) slowly, allowing the crude polymer to precipitate. After filtration, the crude product was subjected to Soxhlet extraction with methanol, hexane and chloroform in sequence. The chloroform fraction was evaporated to dryness and further dried in a vacuum for 1 day to get the final product as a black solid (150 mg, yield: 82%).

### Synthesis of **J12**

A solution of **M2** (151 mg, 0.15 mmol), **M3** (105 mg, 0.15 mmol) in dry toluene (10 mL) and DMF (0.2 mL) was put into a two-necked flask. The solution was flushed with Ar for 20 min and  $\text{Pd}(\text{PPh}_3)_4$  (8 mg) was added into the flask. The solution was flushed with Ar again for 20 min. The oil bath was carefully heated to 110 °C and the reactant was stirred for 6 h at this temperature. After the reaction mixture was cooled to room temperature, the mixture was poured into methanol (150 mL) slowly, allowing the crude polymer to precipitate. After filtration, the crude product was subjected to Soxhlet extraction with methanol, hexane and chloroform in sequence. The chloroform fraction was evaporated to dryness and further dried in a vacuum for 1 day to get the final product as a black solid (130 mg, yield: 70%).



**Scheme S1.** Synthesis route of **m-ITTC**.

### *Synthesis of m-ITTC*

*m*-IDTT-CHO (108 mg, 0.10 mmol), TC (100 mg, 0.5 mmol), chloroform (30 mL), and pyridine (0.5 mL) were added to a two-necked round-bottomed flask. The mixture was deoxygenated with nitrogen for 30 min and then refluxed for 12 h. After cooling to room temperature, the mixture was poured into methanol (200 mL) and filtered. The residue was purified by column chromatography on silica gel using petroleum ether/dichloromethane (1:2) as eluent, yielding a dark blue solid (130 mg, yield: 90%).

<sup>1</sup>H NMR (400 MHz, CDCl<sub>3</sub>): δ 8.81 (s, 2H), 8.37 (d, *J* = 1.9 Hz, 2H), 8.13 (s, 2H), 7.89 (d, *J* = 1.9 Hz, 2H), 7.65 (s, 2H), 7.21 (dd, *J* = 13.8, 6.0 Hz, 8H), 7.12 (d, *J* = 7.5 Hz, 4H), 7.03 (d, *J* = 7.6 Hz, 4H), 2.58 (t, *J* = 7.6 Hz, 8H), 1.62-1.51 (m, 8H), 1.32-1.17 (m, 24H), 0.79 (t, *J* = 6.5 Hz, 12H).

<sup>13</sup>C NMR (75 MHz, CDCl<sub>3</sub>): δ 179.70, 154.75, 154.11, 151.71, 146.18, 146.13, 142.40, 142.26, 141.14, 140.83, 140.24, 138.28, 138.08, 135.72, 135.59, 127.36, 127.16, 126.53, 126.31, 123.98, 123.48, 117.22, 113.66, 112.88, 75.85, 66.33, 62.36, 34.74, 30.33, 30.10, 27.69, 21.26, 12.75, -1.37.

### **Material characterization**

<sup>1</sup>H NMR and <sup>13</sup>C NMR spectra were recorded on Bruker AVANCE 300 MHz or Bruker AVANCE 400 MHz NMR spectrometer at room temperature. Mass spectra were measured on a Shimadzu spectrometer.

The UV-vis absorption spectra were measured on a Hitachi U-3010 UV-vis spectrophotometer. For the preparation of the solution samples, the photovoltaic materials (~1 mg) were dissolved in chloroform (~125 mL) without any aging or filtering procedure. The concentration of the solutions used for the UV-Vis absorption measurement was 10<sup>-2</sup>~10<sup>-3</sup> mg/mL. For the sample of thin films, the films were prepared by spin-coating (2500~3000 rpm) the chloroform solutions (15 mg/mL for neat films, 18 mg/mL for blend films) on quartz plates. The absorption coefficients of the polymer films were obtained by dividing the absorbance by the film thickness. To measure the thickness of thin films, several grooves were firstly marked on the thin film by pointed tweezer, and then the depths of the grooves were recorded on Bruker DEKTAK XT step profiler. The average value of the depths was used as the thickness of thin film.

Cyclic voltammetry was conducted on a Zahner IM6e electrochemical workstation

using sample film coated on glassy carbon as the working electrode, Pt wire as the counter electrode, and Ag/AgCl as the reference electrode, in a 0.1 M tetrabutylammonium hexafluorophosphate ( $\text{Bu}_4\text{NPF}_6$ ) acetonitrile solution. The redox potential of  $\text{Fc}/\text{Fc}^+$  ( $\phi_{\text{Fc}/\text{Fc}^+}$ ) was measured in the same electrolyte solution with Ag/AgCl as the reference electrode for the calculation of HOMO and LUMO energy levels of the polymers. Density functional theory (DFT) calculations at the B3LYP/6-31G (d, p) level were carried out to evaluate the molecular energy levels of the BDT units and polymers.

### **Device fabrication and characterization of the PSCs**

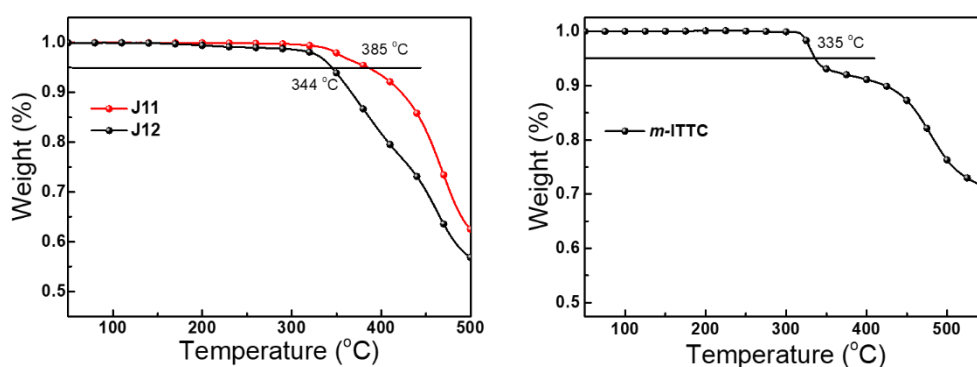
The PSCs were fabricated with a structure of ITO/PEDOT: PSS/active layer/PDINO/Al. The ITO glass was cleaned by sequential ultrasonic treatment in detergent, deionized water, acetone and isopropanol, and then treated in an ultraviolet-ozone chamber (Ultraviolet Ozone Cleaner, Jelight Company, USA) for 20 min. The PEDOT: PSS aqueous solution (Baytron P 4083 from H. C. Starck) was filtered through a 0.45  $\mu\text{m}$  filter and spin-coated on precleaned ITO-coated glass at 4000 rpm for 30 s. Subsequently, the PEDOT: PSS film was baked at 150  $^\circ\text{C}$  for 20 min in air to give a thin film with a thickness of  $\sim 30$  nm. A blend solution of the polymer donor and *m*-ITTC acceptor was prepared by dissolving the donor and acceptor in chloroform ( $\text{CHCl}_3$ ), and then the blend solution was spin-coated at 2500 rpm onto the PEDOT: PSS layer to get the active layer (100~110 nm thickness). Then methanol solution of PDINO at a concentration of 1.0  $\text{mg mL}^{-1}$  was deposited atop the active layer at 3000 rpm for 30 s to afford a PDINO cathode buffer layer. Finally, the metal cathode Al was thermally evaporated under a shadow mask with a base pressure of approximately  $10^{-5}$  Pa. The photovoltaic area of the device is 4.6  $\text{mm}^2$ . Optical microscope (Olympus BX51) was used to define the active area of the devices.

The current density-voltage ( $J$ - $V$ ) characteristics of the PSCs were measured in a nitrogen glove box with a Keithley 2450 Source Measure unit. Oriel Sol3A Class AAA Solar Simulator (model, Newport 94023A) with a 450W xenon lamp and an air mass (AM) 1.5 filter was used as the light source. The light intensity was calibrated to 100  $\text{mW cm}^{-2}$  by a Newport Oriel 91150V reference cell. The input photon to converted current efficiency (IPCE) was measured by Solar Cell Spectral Response Measurement System QE-R3-011 (Enli Technology Co., Ltd., Taiwan). The light intensity at each wavelength was calibrated with a standard single-crystal Si photovoltaic cell.

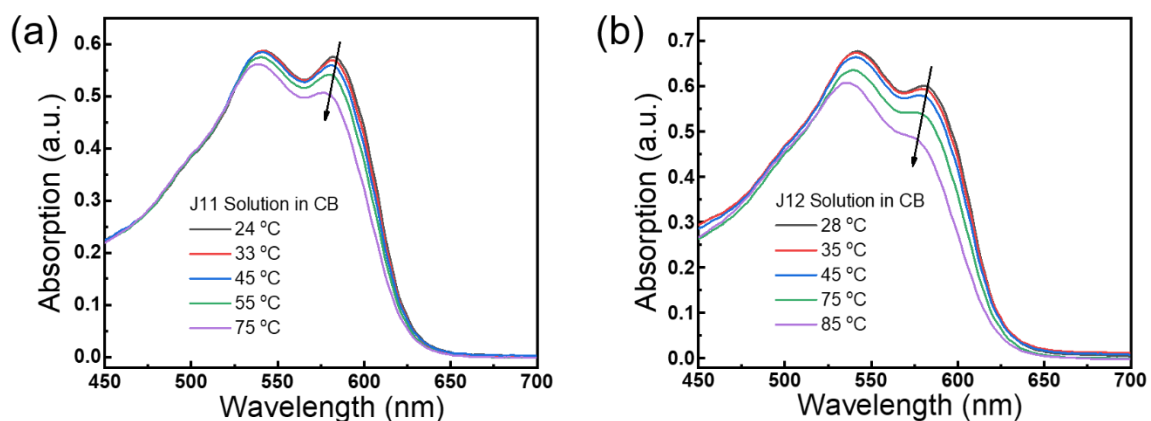
### **Measurement of charge carrier mobilities**

The charge carrier mobilities were measured with the device structure of

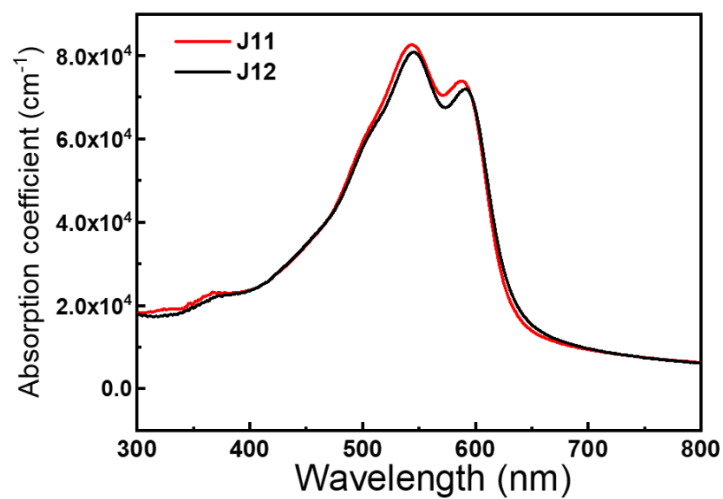
ITO/PEDOT:PSS/active layer/Au (device structure of ITO/PEDOT:PSS/active layer/MoO<sub>3</sub>/Ag were used to measure the thickness-dependent hole mobility) for hole-mobility and ITO/ZnO/active layer/PDINO/Al for electron-mobility. The hole and electron mobilities are calculated according to the space charge limited current (SCLC) method equation:  $J = 9\mu\epsilon_r\epsilon_0 V^2/8d^3$ , where  $J$  is the current density,  $\mu$  is the hole or electron mobility,  $V$  is the internal voltage in the device,  $\epsilon_r$  is the relative dielectric constant of active layer material,  $\epsilon_0$  is the permittivity of empty space, and  $d$  is the thickness of the active layer.



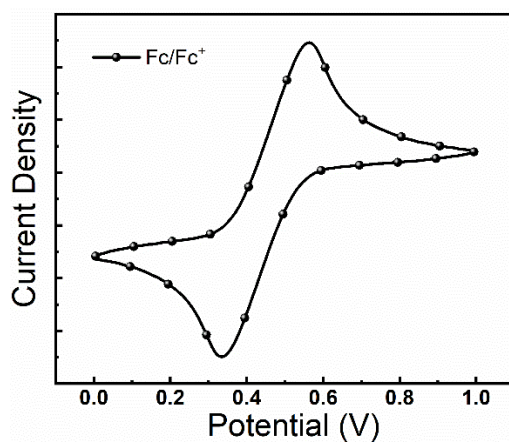
**Figure S1.** TGA plots of J11, J12 and *m*-ITTC with a heating rate of 10 °C min<sup>-1</sup> under an inert atmosphere.



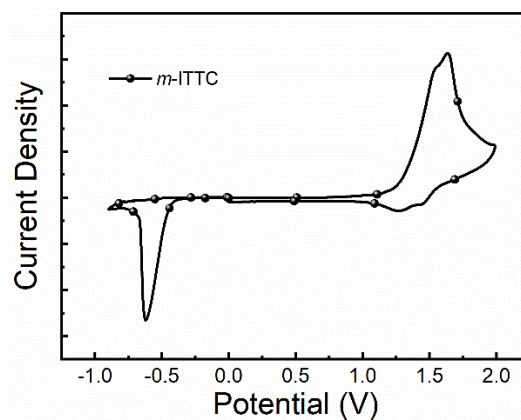
**Figure S2.** Temperature-dependent UV-Vis absorption spectra of J11 and J12 in CB solutions.



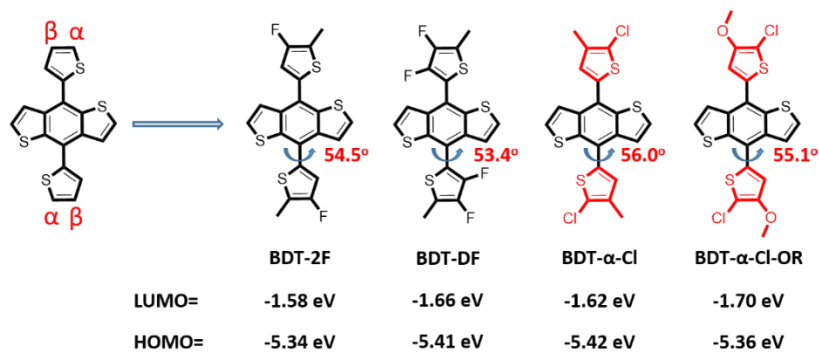
**Figure S3.** Absorption spectra of neat J11 and J12 films.



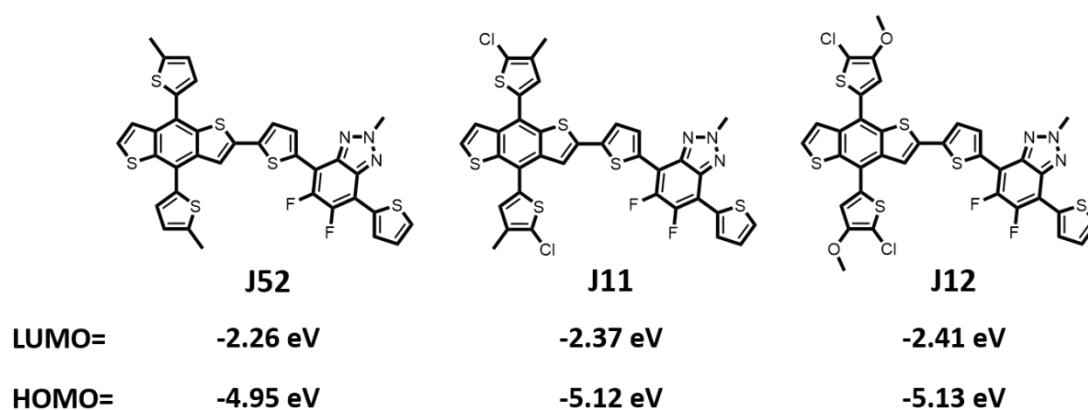
**Figure S4.** Cyclic voltammogram of Fc/Fc<sup>+</sup> with the Ag/AgCl reference electrode.



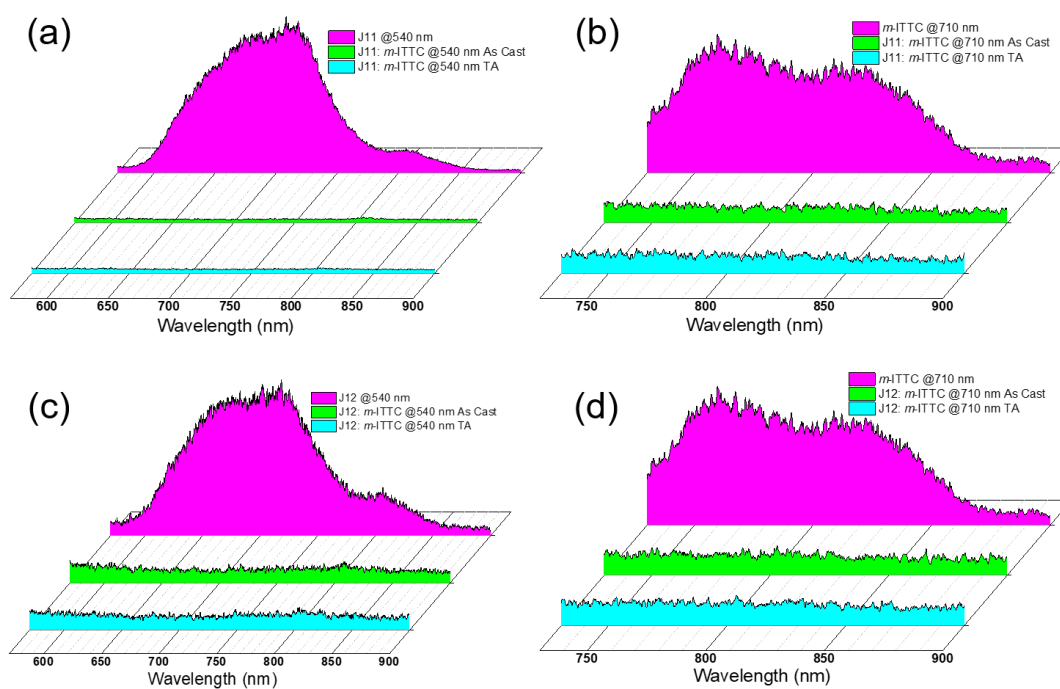
**Figure S5.** Cyclic voltammogram of *m*-ITTC with the Ag/AgCl reference electrode.



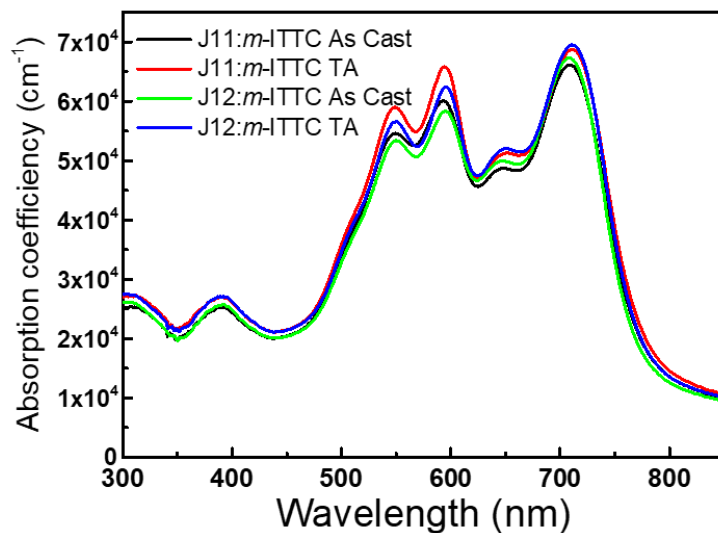
**Figure S6.** HOMO and LUMO energy levels of the selected BDT units estimated by DFT calculation.



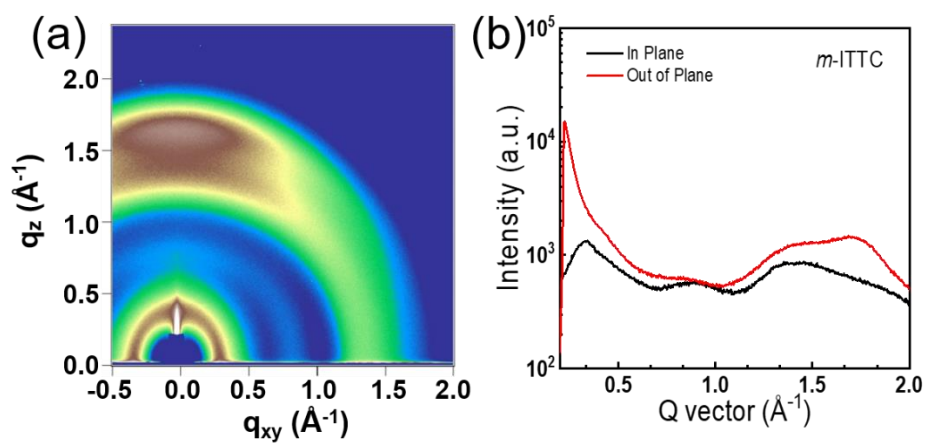
**Figure S7.** HOMO and LUMO energy levels of J52, J11 and J12 estimated by DFT calculation.



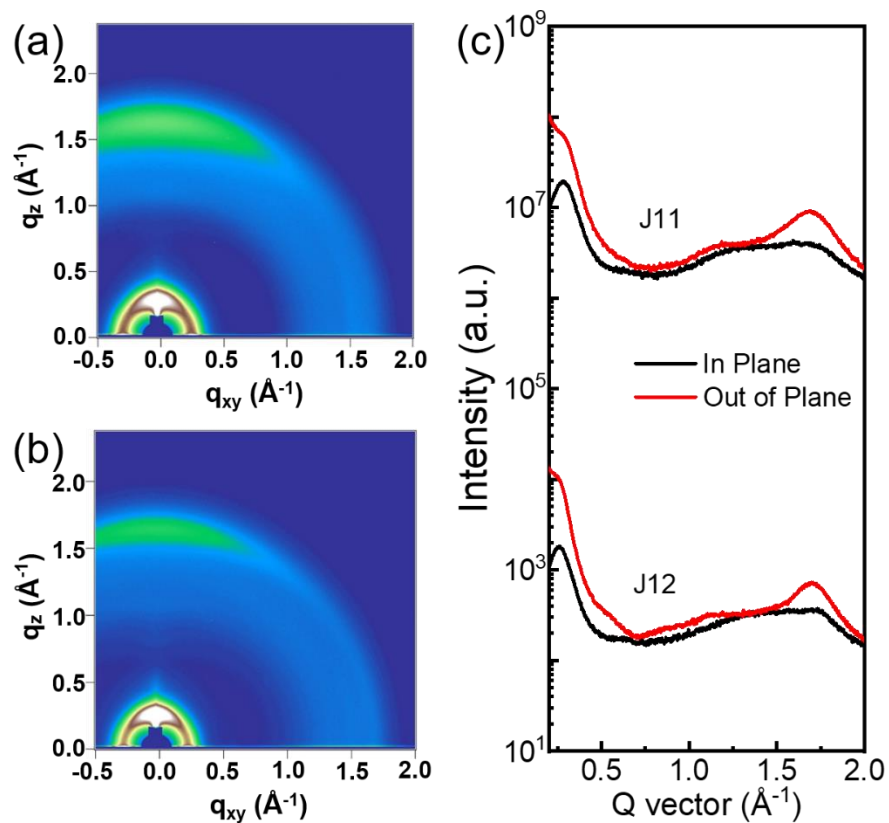
**Figure S8.** Photoluminescence spectra of neat J11, J12 and *m*-ITTC films as well as the blend films of J11: *m*-ITTC and J12: *m*-ITTC with or without thermal annealing treatment.



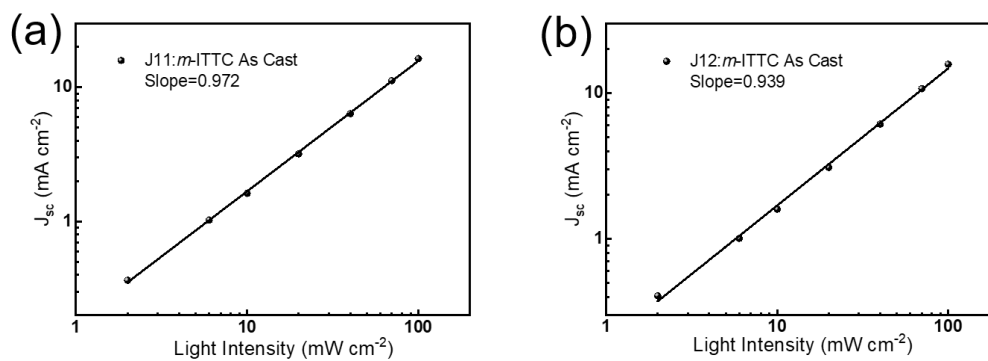
**Figure S9.** Absorption spectra of the blend films of J11: *m*-ITTC and J12: *m*-ITTC with or without thermal annealing treatment.



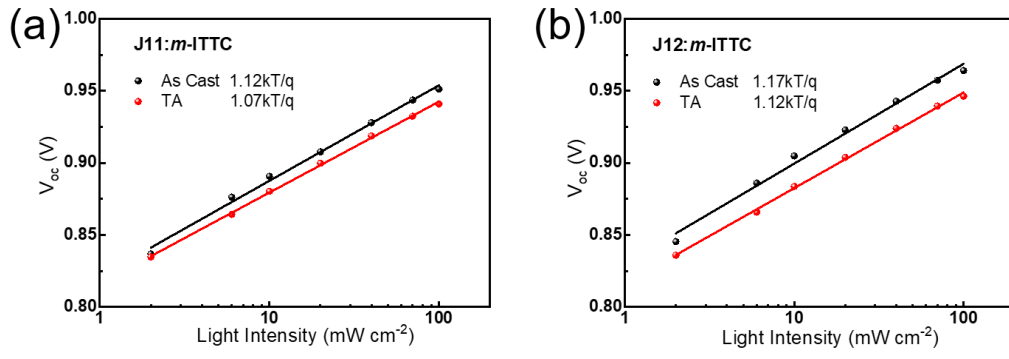
**Figure S10.** GIWAXS image and corresponding in-plane and out-of-plane line cuts of the GIWAXS image of neat *m*-ITTC film.



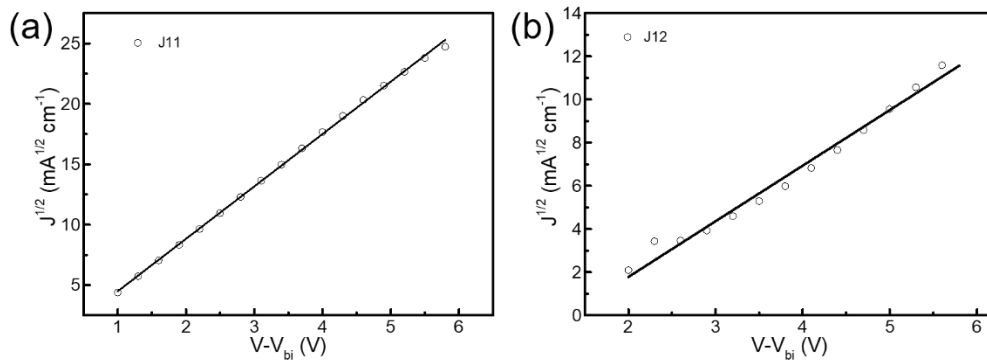
**Figure S11.** GIWAXS images and corresponding in-plane and out-of-plane line cuts of the GIWAXS images of neat J11 and J12 films.



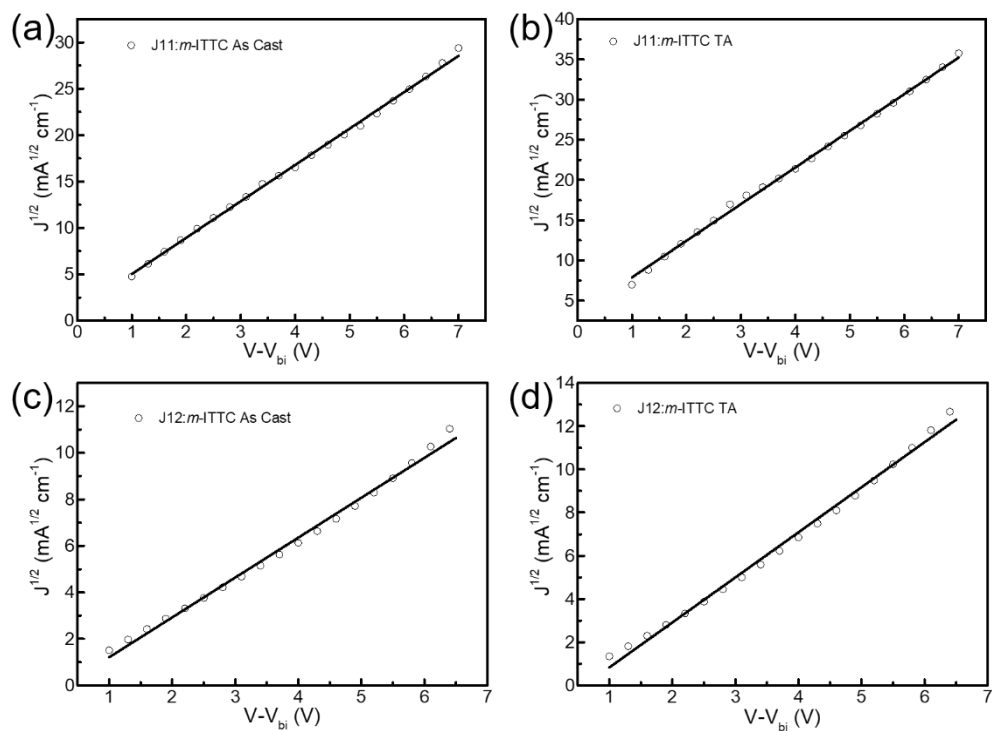
**Figure S12.** Light intensity dependence of  $J_{sc}$  of the devices based on J11: *m*-ITTC and J12: *m*-ITTC blend films.



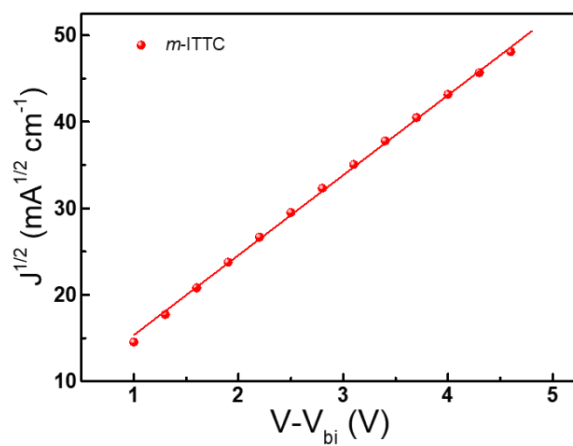
**Figure S13.** Light intensity dependence of  $V_{oc}$  of the devices based on J11: *m*-ITTC and J12: *m*-ITTC blend films.



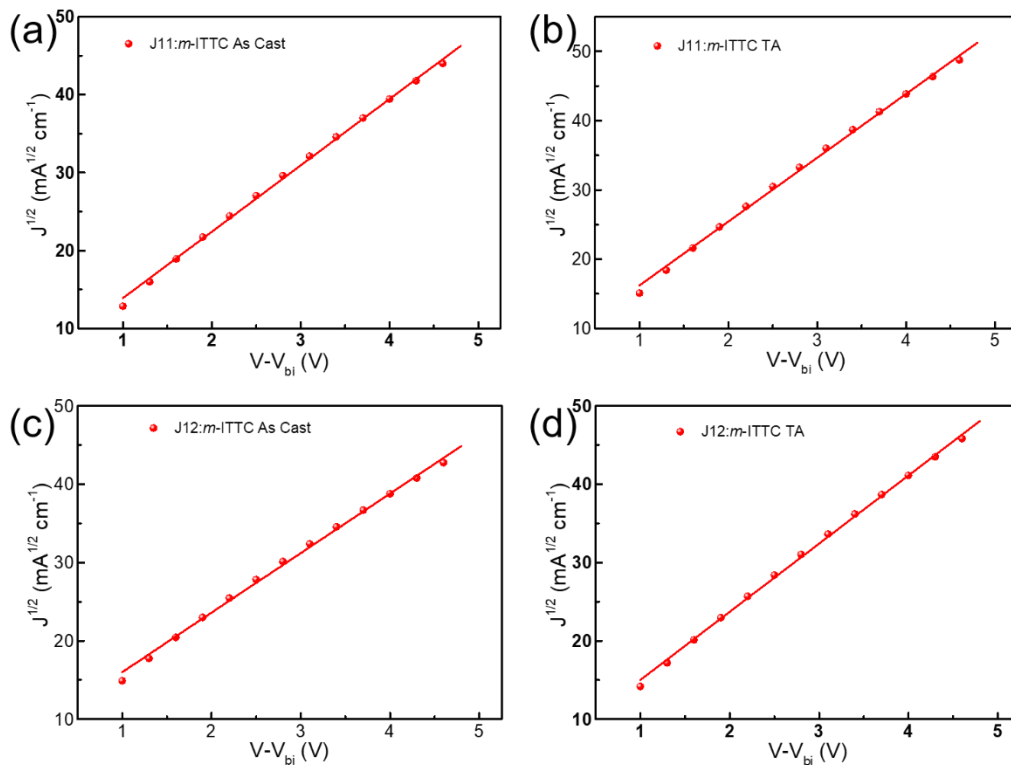
**Figure S14.**  $J$ - $V$  characteristics in the dark for the electron-only devices based on neat J11 and J12 films.



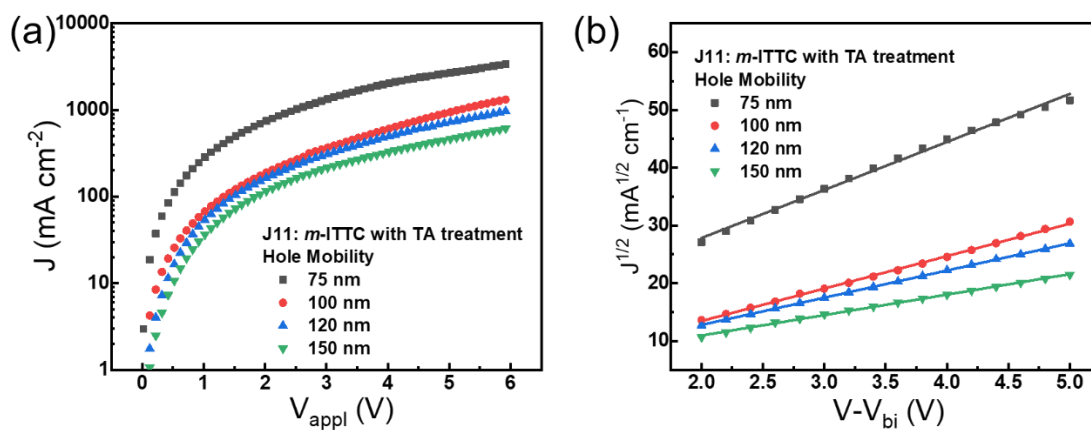
**Figure S15.**  $J$ - $V$  characteristics in the dark for the hole-only devices based on J11:  $m$ -ITTC and J12:  $m$ -ITTC blend films.



**Figure S16.**  $J$ - $V$  characteristics in the dark for the electron-only devices based on neat  $m$ -ITTC film.



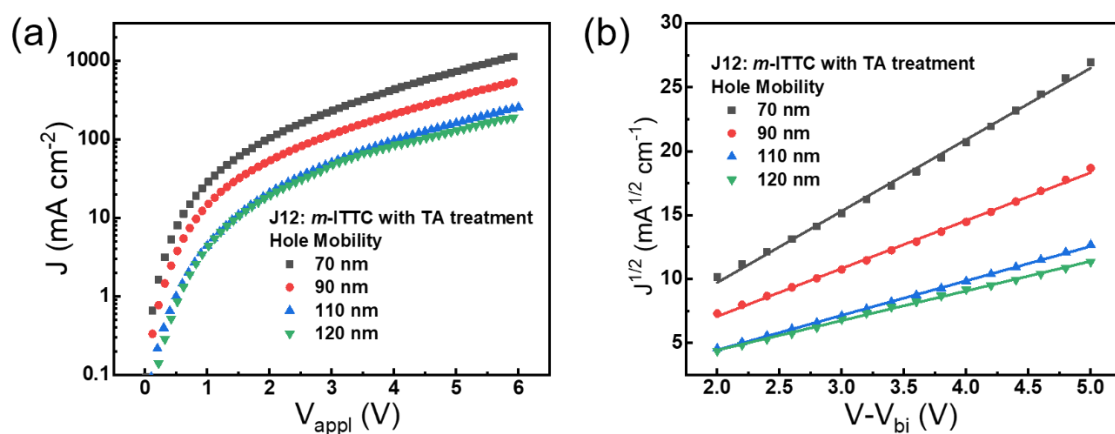
**Figure S17.**  $J$ - $V$  characteristics in the dark for the electron-only devices based on J11:  $m$ -ITTC and J12:  $m$ -ITTC blend films.



**Figure S18.**  $J$ - $V$  characteristics in the dark for the hole-only devices (ITO/PEDOT:PSS/ J11:  $m$ -ITTC/MoO<sub>3</sub>/Ag) based on J11:  $m$ -ITTC blend films with different thickness.

**Table S1.** Hole mobility of the J11: *m*-ITTC blend films with different thickness.

Thickness of J11: <i>m</i> -ITTC blend films	Hole mobility
80 nm	$1.186 \times 10^{-4}$
100 nm	$1.057 \times 10^{-4}$
120 nm	$1.283 \times 10^{-4}$
150 nm	$1.384 \times 10^{-4}$

**Figure S19.**  $J$ - $V$  characteristics in the dark for the hole-only devices (ITO/PEDOT:PSS/ J12: *m*-ITTC/MoO<sub>3</sub>/Ag) based on J12: *m*-ITTC blend films with different thickness.**Table S2.** Hole mobility of the J12: *m*-ITTC blend films with different thickness.

Thickness of J12: <i>m</i> -ITTC blend films	Hole mobility
70 nm	$0.359 \times 10^{-4}$
90 nm	$0.343 \times 10^{-4}$
110 nm	$0.325 \times 10^{-4}$
120 nm	$0.311 \times 10^{-4}$

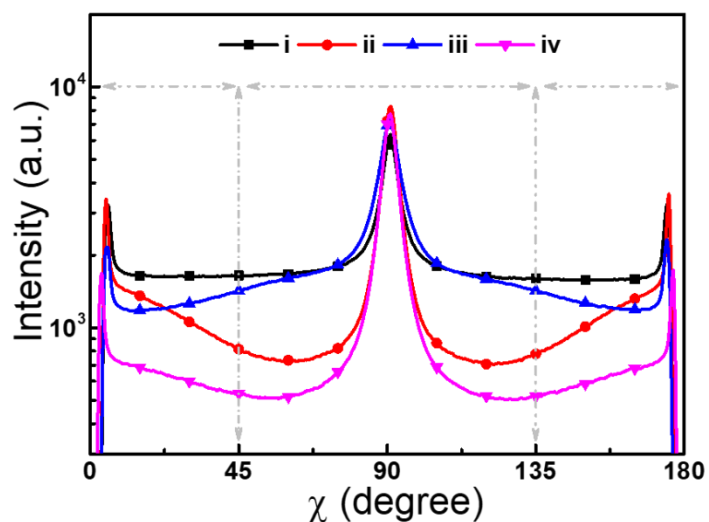


**Figure S20.** Pole figure plots from the (100) lamellar diffraction of polymer: *m*-ITTC films at out-of-plane direction: (i) J11: *m*-ITTC as cast, (ii) J11: *m*-ITTC with TA treatment, (iii) J12: *m*-ITTC as cast, (iv) J11: *m*-ITTC with TA treatment.

**Table S3.** Photovoltaic performance parameters of the PSCs based on J11: *m*-ITTC (1:1, w/w) and J12: *m*-ITTC (1:1, w/w) with different TA treatment condition.

Active layer	TA condition	$V_{oc}$ (V)	$J_{sc}$ (mA cm <sup>-2</sup> )	FF (%)	PCE (%)
J11: <i>m</i> -ITTC	130 °C 2 min	0.939	17.92	71.8	12.08
	150 °C 1 min	0.935	18.05	73.0	12.32
	150 °C 2 min	0.933	18.27	71.0	12.10
J12: <i>m</i> -ITTC	130 °C 2 min	0.951	16.86	54.1	8.68
	150 °C 1 min	0.943	16.64	55.7	8.74
	150 °C 2 min	0.934	16.45	51.9	7.98

**Table S4.** Photovoltaic performance parameters of the PSCs based on J11: *m*-ITTC and J12: *m*-ITTC with different D/A ratio.

Active layer	D/A ratio	$V_{oc}$ (V)	$J_{sc}$ (mA cm <sup>-2</sup> )	FF (%)	PCE (%)
J11: <i>m</i> -ITTC	1:1.5	0.928	17.61	70.4	11.51
	1:1	0.935	18.05	73.0	12.32
	1.5:1	0.933	18.31	68.4	11.68
	1:1.5	0.935	15.76	56.3	8.30
J12: <i>m</i> -ITTC	1:1	0.943	16.64	55.7	8.74
	1.5:1	0.946	16.48	54.8	8.55

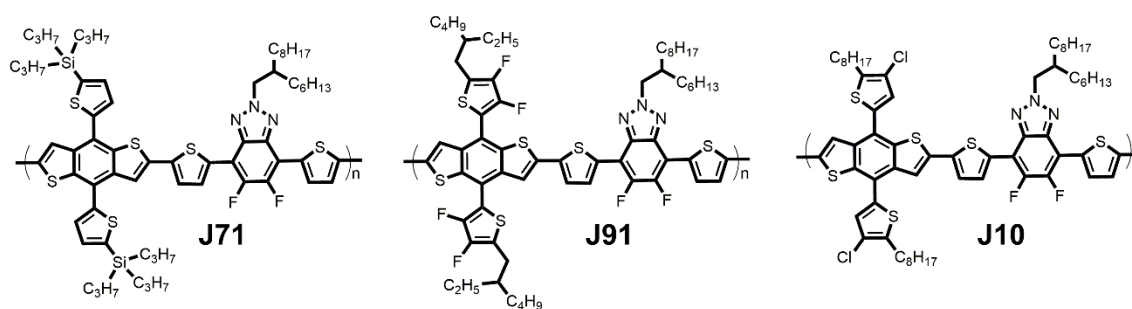


**Figure S21.** Molecular structures of the polymers used for comparison.

**Table S5.** Photovoltaic performance parameters of the PSCs based on J-series polymers: *m*-ITTC

Active layer	$V_{oc}$ (V)	$J_{sc}$ (mA cm <sup>-2</sup> )	FF (%)	PCE (%)	$J_{sc}^a$ (mA cm <sup>-2</sup> )
J71: <i>m</i> -ITTC	0.892	18.42	68.7	11.29	18.06
J91: <i>m</i> -ITTC	0.930	18.32	61.4	10.46	18.01
J10: <i>m</i> -ITTC	0.848	17.81	57.8	8.73	17.41
J11 <sup>b</sup> : <i>m</i> -ITTC	0.920	18.62	70.9	12.15	18.28

<sup>a</sup> calculated from IPCE.

<sup>b</sup> High molecular weight with  $M_n$  of 34.8 KDa and  $M_w$  of 60.6 KDa.

**MW Averages**

Mp: 33085      Mn: 18769      Mv: 31532      Mw: 33922  
Mz: 51376      Mz+1: 68680      PD: 1.8073

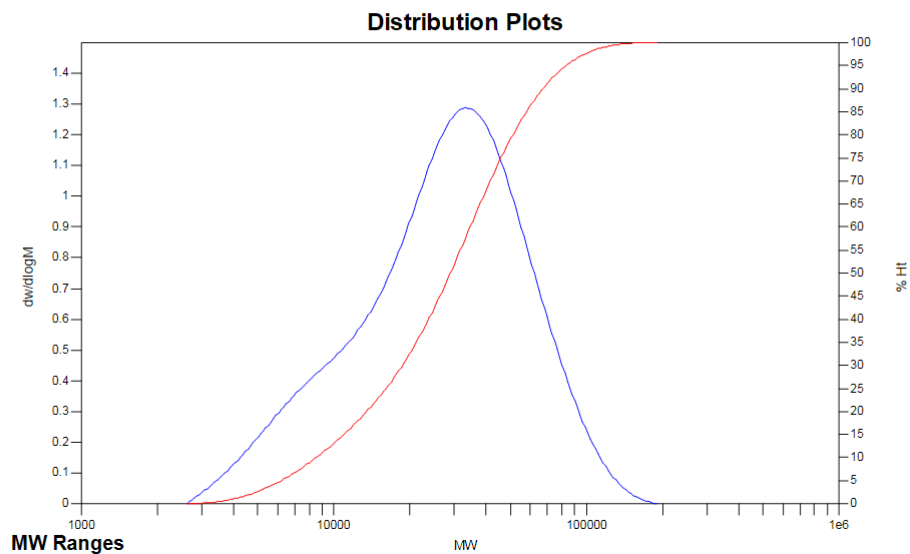


**Figure S22.** High-temperature gel permeation chromatography plots of polymer J11.

**MW Averages**

Mp: 33085      Mn: 31883      Mv: 39280      Mw: 40772  
Mz: 51881      Mz+1: 64082      PD: 1.2788

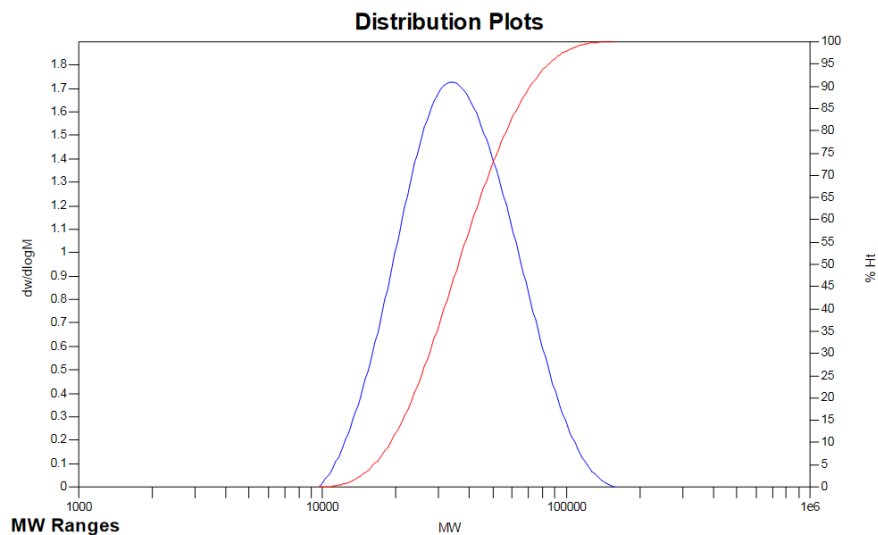


**Figure S23.** High-temperature gel permeation chromatography plots of polymer J12.

**MW Averages**

Mp: 45840

Mn: 34817

Mv: 55999

Mw: 60550

Mz: 97182

Mz+1: 138604

PD: 1.7391

**Distribution Plots**

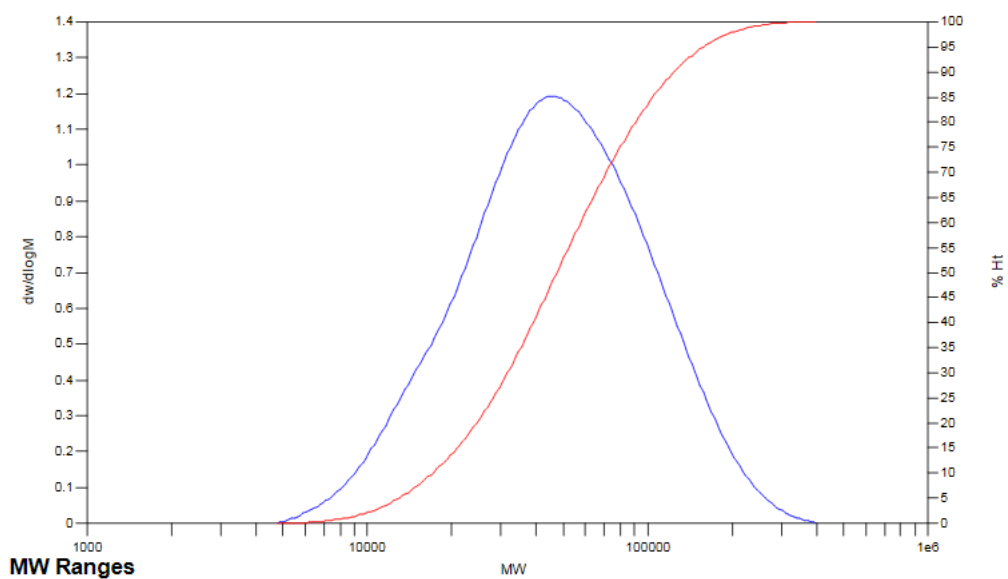


**Figure S24.** High-temperature gel permeation chromatography plots of polymer J11 (high molecular weight).

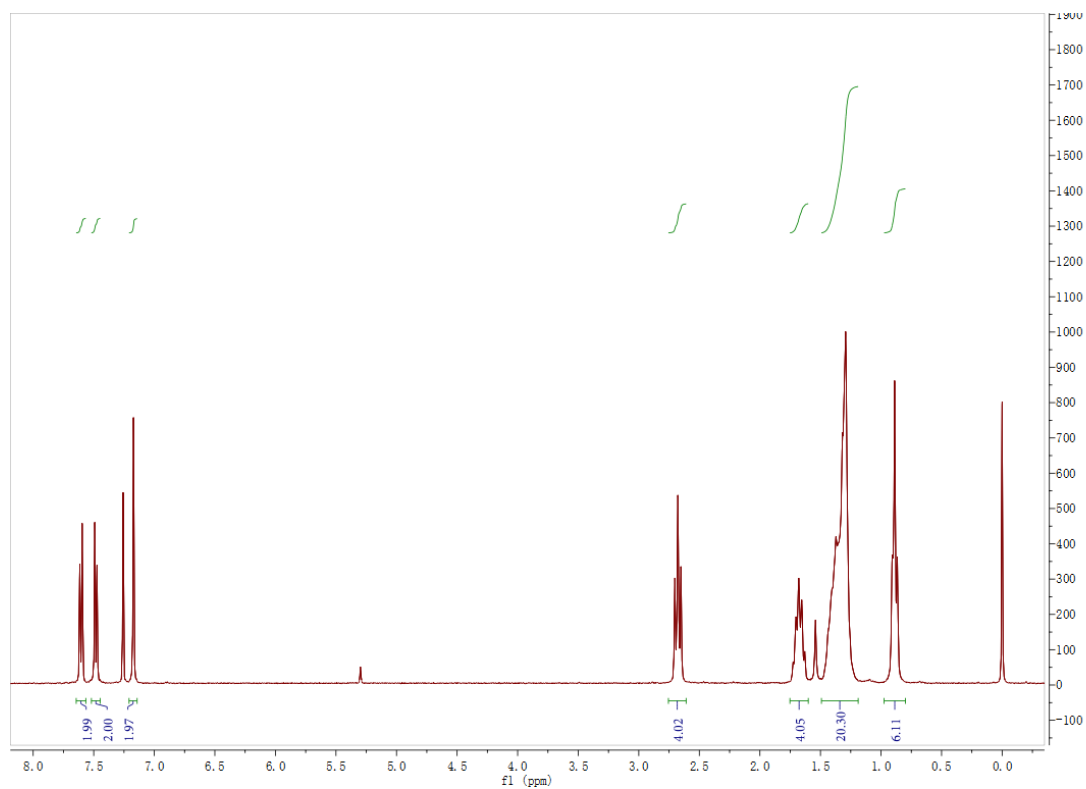


**Figure S25.**  $^1\text{H}$  NMR spectrum of 3a

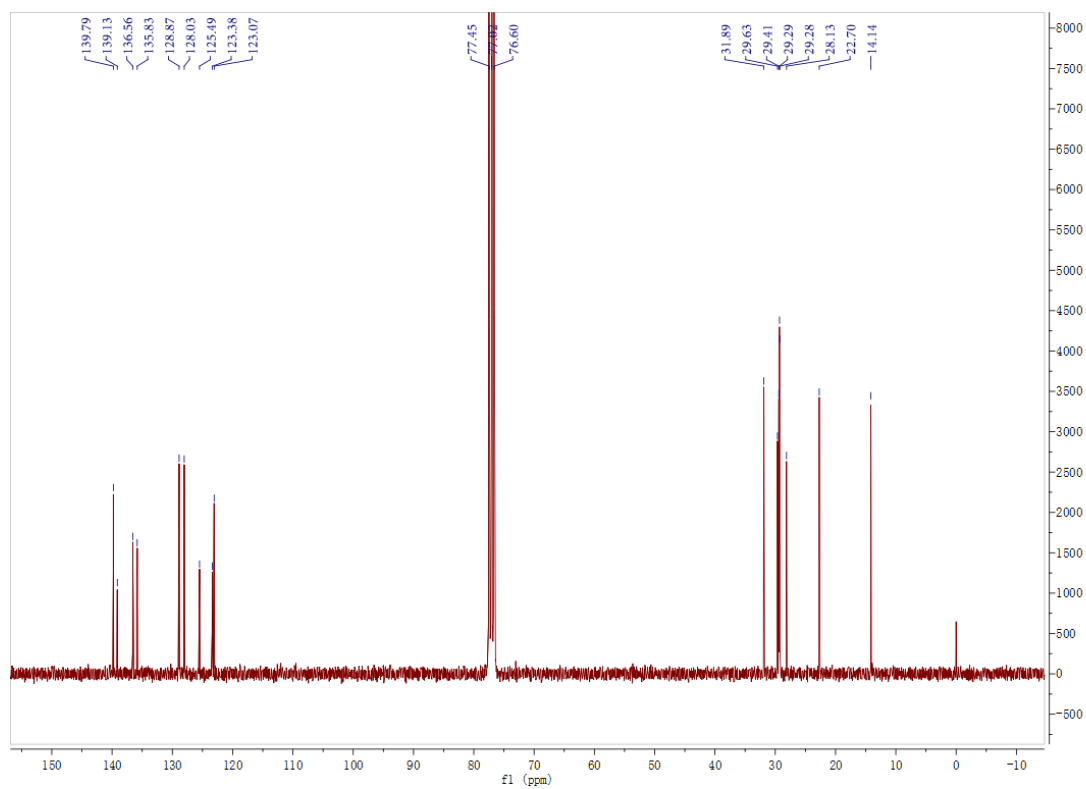


Figure S26.  $^{13}\text{C}$  NMR spectrum of 3a

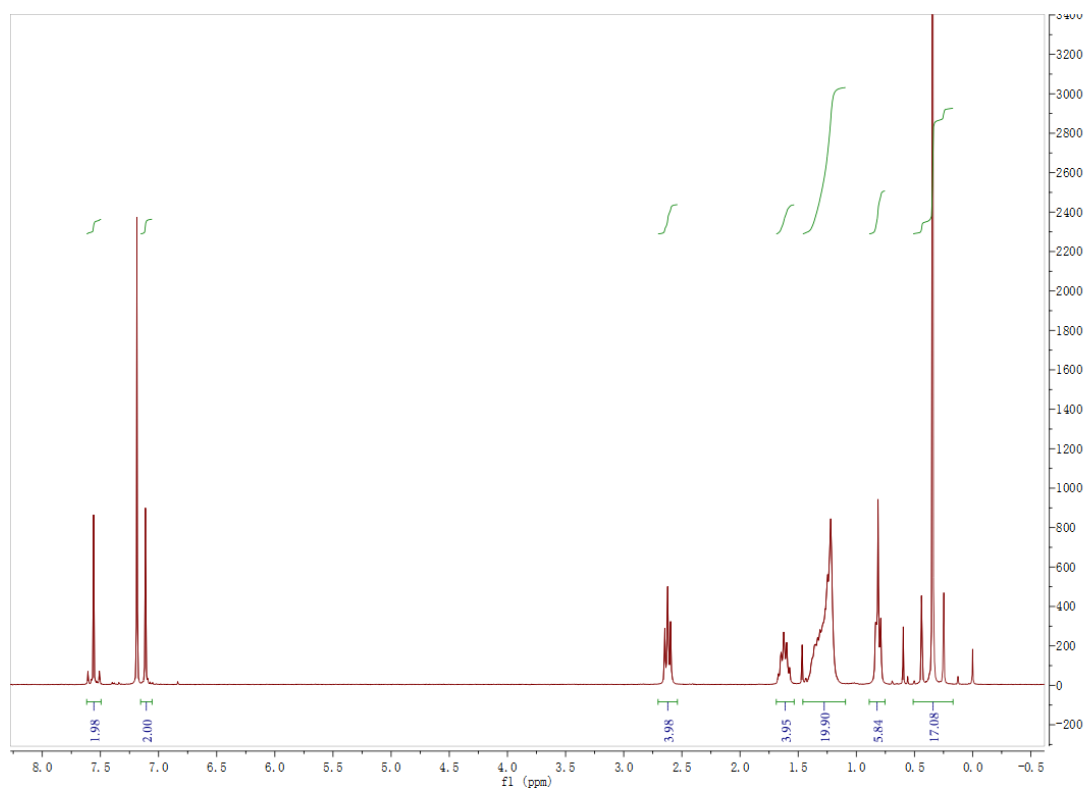
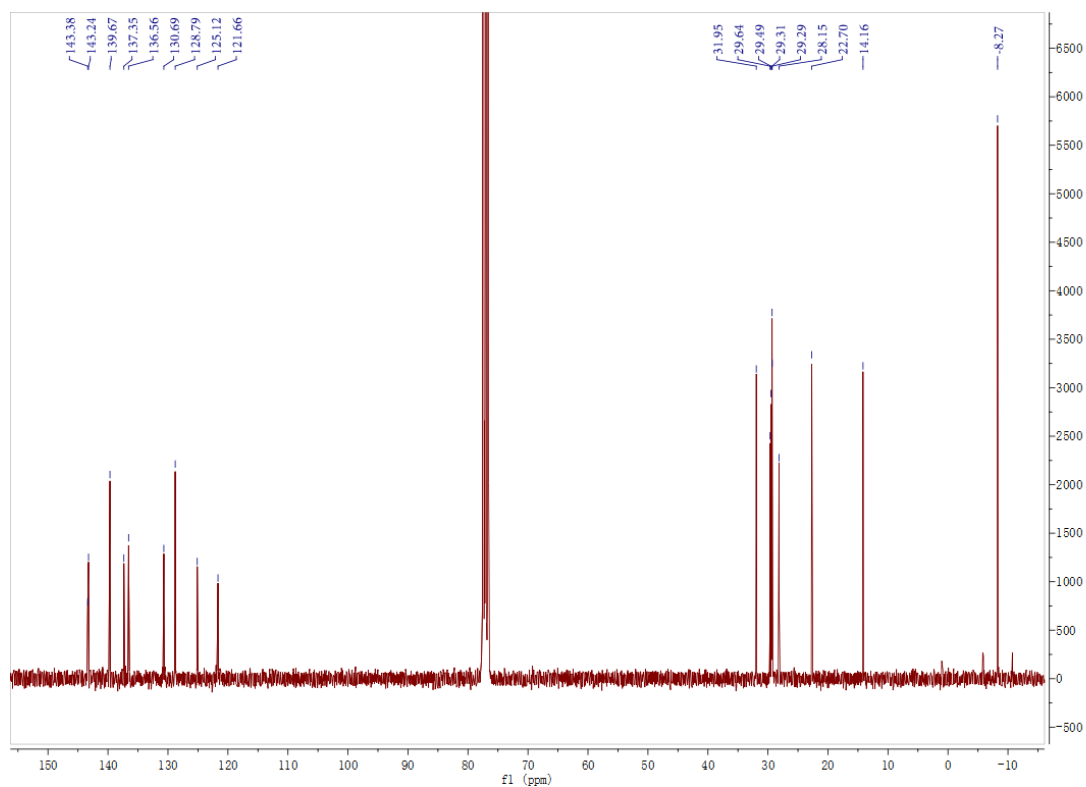
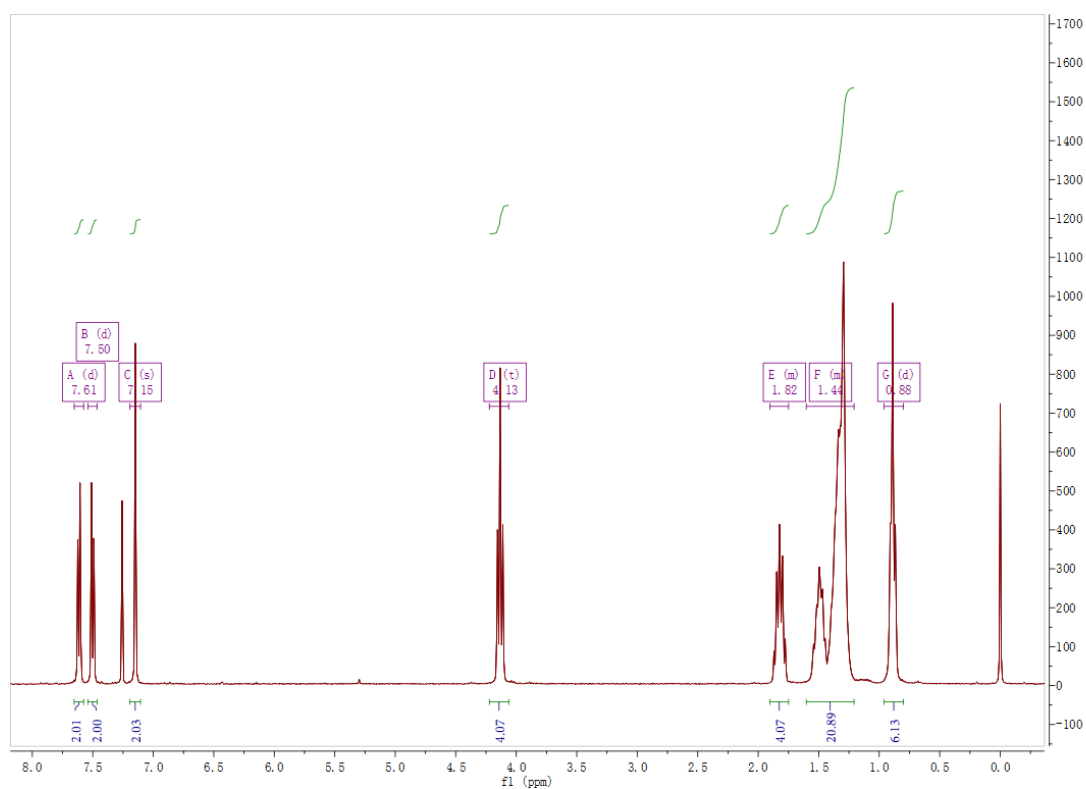


Figure S27.  $^1\text{H}$  NMR spectrum of M1



**Figure S28.**  $^{13}\text{C}$  NMR spectrum of M1



**Figure S29.**  $^1\text{H}$  NMR spectrum of 3b

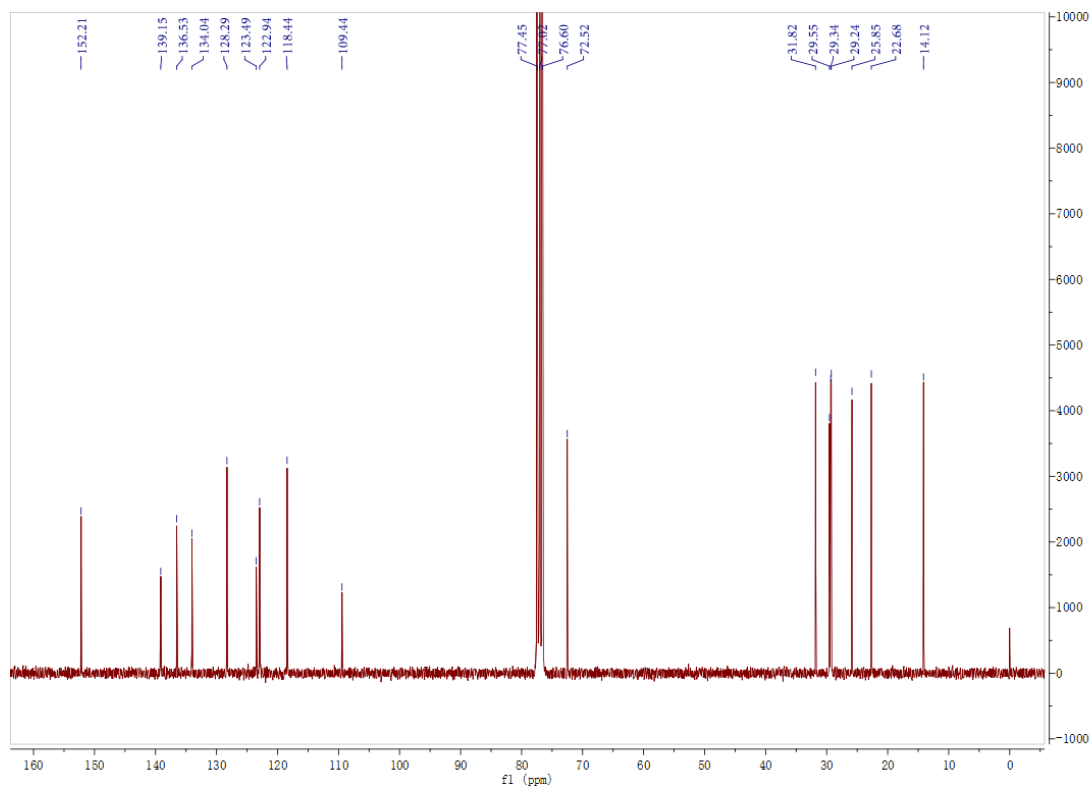


Figure S30. <sup>13</sup>C NMR spectrum of 3b

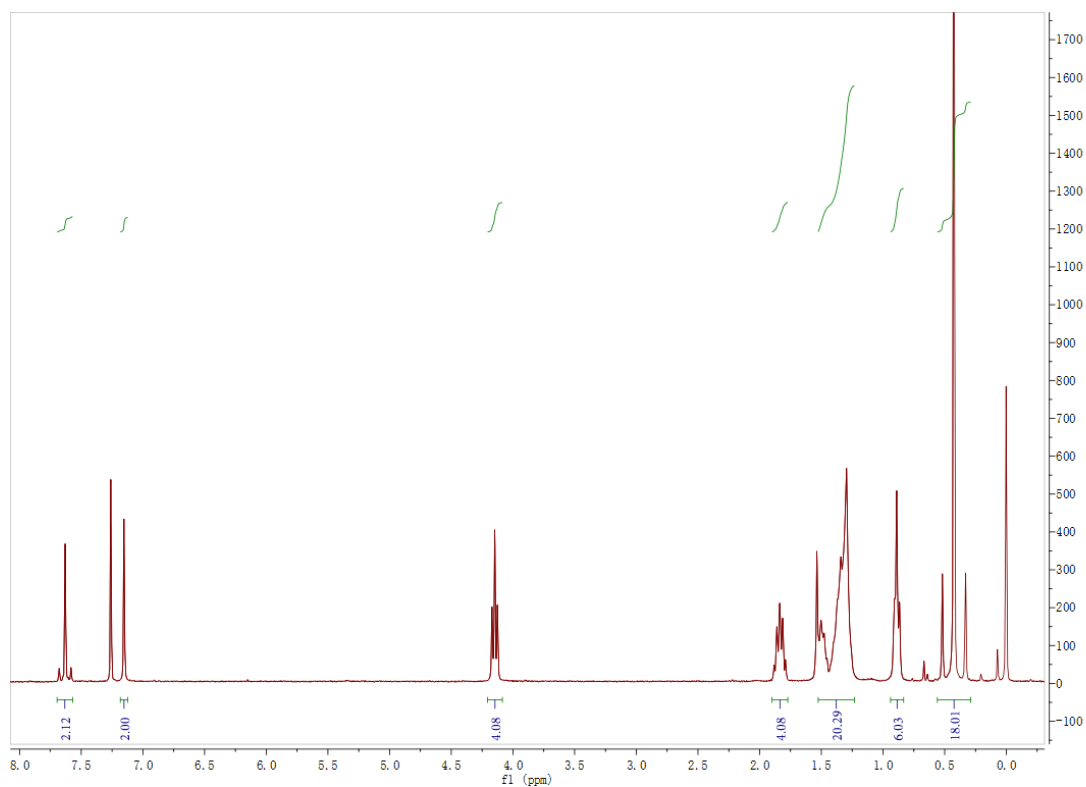


Figure S31. <sup>1</sup>H NMR spectrum of M2

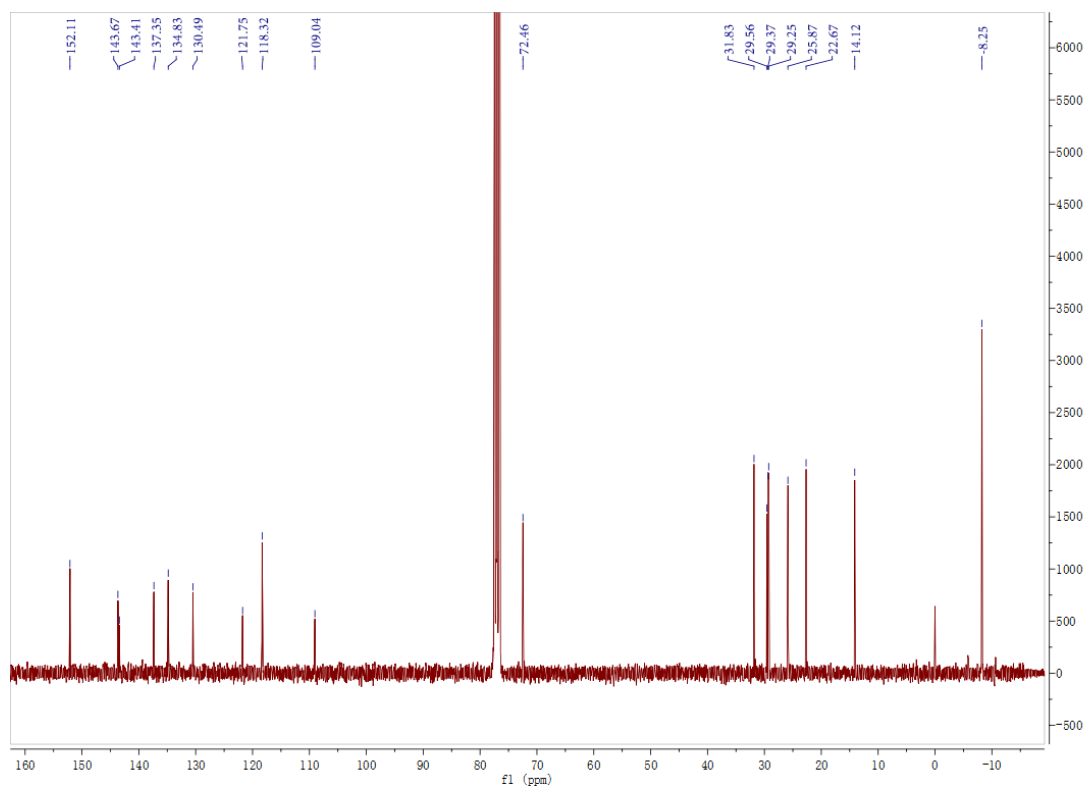


Figure S32. <sup>13</sup>C NMR spectrum of M2

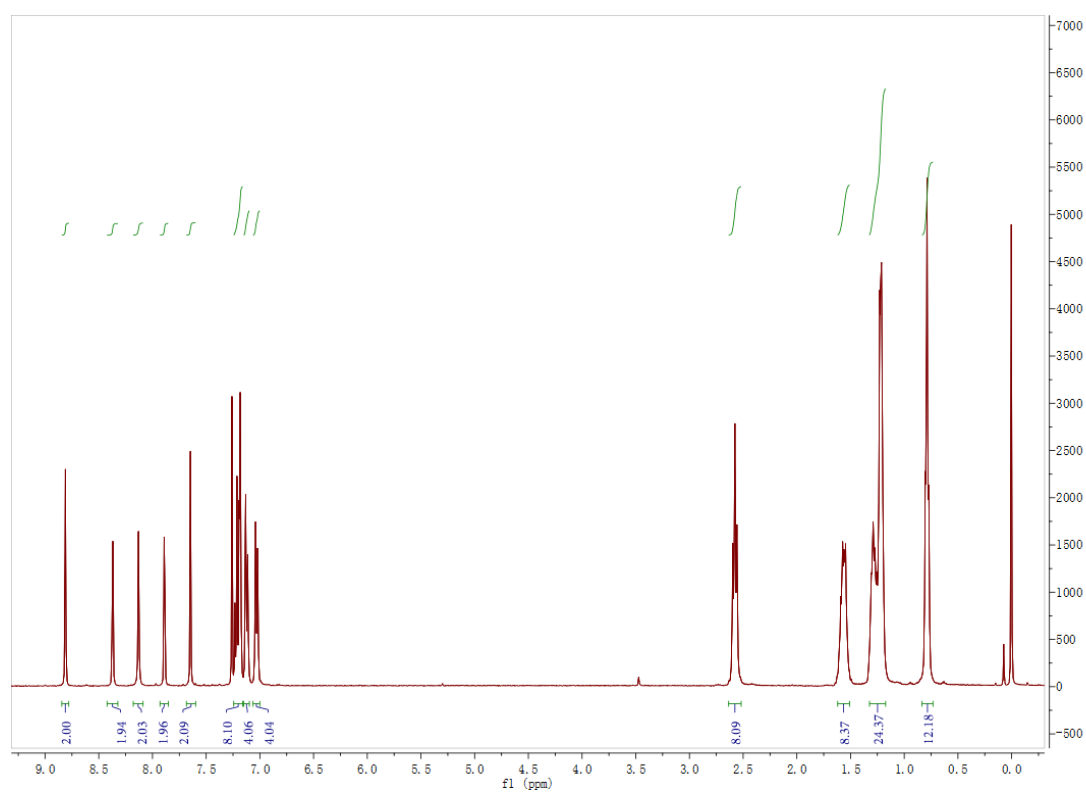


Figure S33. <sup>1</sup>H NMR spectrum of *m*-ITTC

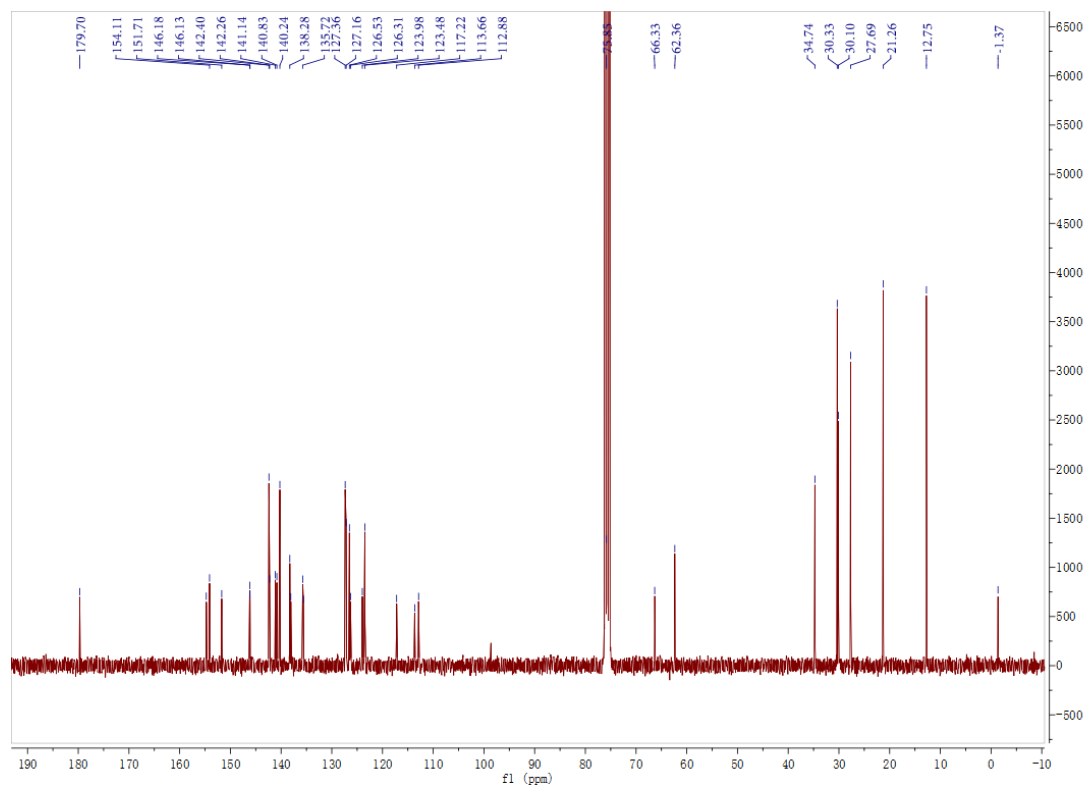


Figure S34.  $^{13}\text{C}$  NMR spectrum of *m*-ITTC